

## Localized-to-extended-states transition below the Fermi level

M. A. Tito and Yu. A. Pusep

*São Carlos Institute of Physics, University of São Paulo, P.O. Box 369, 13560-970 São Carlos, São Paulo, Brazil*

(Received 5 December 2017; revised manuscript received 13 March 2018; published 7 May 2018)

Time-resolved photoluminescence is employed to examine a transition from localized to extended electron states below the Fermi level in multiple narrow quantum well GaAs/AlGaAs heterostructures, where disorder was generated by interface roughness. Such a transition resembles the metal-insulator transition profoundly investigated by electric transport measurements. An important distinction distinguishes the localized-to-extended-states transition studied here: it takes place below the Fermi level in an electron system with a constant concentration, which implies unchanging Coulomb correlations. Moreover, for such a localized-to-extended-states transition the temperature is shown to be irrelevant. In the insulating regime the magnetic field was found to cause an additional momentum relaxation which considerably enhanced the recombination rate. Thus, we propose a method to explore the evolution of the localized electron states in a system with a fixed disorder and Coulomb interaction.

DOI: [10.1103/PhysRevB.97.184203](https://doi.org/10.1103/PhysRevB.97.184203)

### I. INTRODUCTION

The subject of metal-insulator transition (MIT) has experienced a renewed focus in the last decade due to recent achievements: evidence of the formation of a complex structure around the MIT giving rise to strongly inhomogeneous states and to several intermediate phases [1], understanding of the deep significance of the strong correlations physics [2], and progress in understanding the MIT in the frame of the concept of quantum phase transition which takes place at absolute zero temperature and which is governed by the zero-point quantum fluctuations [3]. The MIT manifests in electric transport measurements. In the presence of the MIT these measurements reveal either a drastic drop in the conductivity below a certain critical electron concentration or a change in the temperature dependence of the conductivity from a metallic behavior to an insulating one which takes place at this critical concentration. Such a performance of the electric conductivity is well understood in terms of the mobility edge, the energy which separates the localized states below from the high-energy extended states above [4,5]. The insulating phase corresponds to an electron system with the Fermi level below the mobility edge. The increasing electron concentration (by doping or electric/optical injection) causes the Fermi level to increase. A transition to a metallic phase occurs when the Fermi level passes the mobility edge. However, any variation of the electron concentration radically changes the Coulomb correlation among electrons, adding an additional variable to the theoretical analysis of the MIT phenomena. In such a case, considerable improvement may be achieved by examining the modification of the electron states in a disordered system with a constant electron concentration. Recently, we demonstrated the fundamental connection between the mobility edge of excitons and localization properties of the conduction-band electrons [6]. Using the time-resolved photoluminescence (PL) technique we studied the recombination rate of the electrons photoexcited in a conduction-band disordered potential.

According to Fermi's golden rule, the recombination rate determines the transition probability between the initial and final states, and thus, it gives direct access to the electron states participating in the transition. Therefore, any modification of the electron states must influence the recombination rate. In this work we employ the time-resolved PL as a tool to study a change in the character of the electron states across the mobility edge. The electrons residing below the mobility edge energy are localized and, consequently, recombine with the holes over a longer time relative to the extended electrons above the mobility edge. The recombination time significantly changes at the energy of the mobility edge, which therefore can be determined. In contrast to the electric measurements which probe the electrons in close proximity to the Fermi surface, all the conduction-band electron states below the Fermi level contribute to PL independently of the relative position of the mobility edge. In such a case the transmutation of extended electron states into localized states may be explored in one sample (either metallic or insulating) without alteration of the electron concentration. Furthermore, in the metallic regime the mobility edge is located below the Fermi level. Given that, the transition from localized to extended states takes place in the range of the occupied conduction-band states, and therefore, it does not depend on the temperature. Thus, the time-resolved spectroscopic measurements provide a probe for dynamic properties of the electrons below the Fermi level which provides an important advantage compared to electric transport measurements: the mobility edge and a character of the electron states may be determined at a constant electron density which therefore does not change the Coulomb correlation in the system.

In the present work we report on the use of a high magnetic field to study a localization-extended transformation of the electron states below the Fermi level in a quasi-two-dimensional electron system which undergoes the disorder-driven MIT. The disorder is produced by interface roughness. The scattering due to short-range interface roughness was

predicted to cause the disorder-induced MIT in Ref. [7]. In our earlier article [8] we demonstrated the MIT governed by interface roughness in GaAs/AlGaAs multiple quantum wells in which variation of the quantum well width was used to control the strength of the scattering. With the decreasing quantum well width the effect of the interface imperfections begins to dominate the parallel transport, resulting in an insulating regime at a critical quantum well width. In this paper the time-resolved PL is studied in the same structures as a function of the temperature and the magnetic field. An expected shift of the mobility edge to higher energy is observed in the metallic samples due to the magnetic field quantization of the conduction-band electron energy. However, in the insulating samples the magnetic field is found to cause a significant relaxation of the momentum selection rule which enhances the probability of recombination of the localized electrons with the valence-band photoexcited holes. Thus, magnetic-field-induced modification of the localized electron state in the momentum space is demonstrated.

## II. EXPERIMENTAL DETAILS

The samples studied here are  $(\text{GaAs})_m(\text{Al}_{0.3}\text{Ga}_{0.7}\text{As})_n$  multiple quantum wells (MQWs) uniformly doped with Si, where  $m$  and  $n$  are the thicknesses of corresponding layers expressed in monolayers (ML). A total of 30 quantum wells were grown by molecular beam epitaxy on the (001) semi-insulating GaAs substrates. All the samples were doped with the same nominal concentration of Si, which forms the Fermi gas of the conductive electrons. The disordered potential required for the localization is produced by the interface roughness that is always present at the semiconductor heterointerface. The effect of the interface imperfections dominates the parallel transport in thin quantum wells, while it vanishes with increasing quantum well width. Thus, control of the electron conductivity necessary to achieve the MIT is provided. In all the samples the  $\text{Al}_{0.3}\text{Ga}_{0.7}\text{As}$  barriers between the quantum wells were  $n = 6$  ML thick, while a variation of the GaAs quantum well thickness  $m$  in the range 10–150 ML ensures the interface-roughness-disorder-driven MIT. The details of the sample characterization may be found in Refs. [6,8]. According to the magnetotransport measurements [8], structures with 150, 50, 30, and 15 ML reveal metallic behavior, while the 10-ML-thick quantum well shows the insulating regime.

PL and time-resolved PL measurements were performed in the temperature range 1.6–80 K and in the range of the magnetic field from 0 to 10 T applied perpendicular to the interface plane. The samples were excited by a diode laser (PicoQuant LDH-730) emitting at 470 nm in the continuous mode. The PL was collected by an Ocean Optics HR4000 high-resolution spectrometer. The same laser generated 70-ps pulses at a frequency of 80 MHz for time-resolved PL measurements. The PL emission was dispersed by a SPEX500M spectrometer, and the PL time delay was detected by a Hamamatsu H10330B-75 photomultiplier tube.

## III. RESULTS AND DISCUSSION

Typical PL spectra measured from metallic and insulating samples are shown in Fig. 1. The PL peak at an energy of

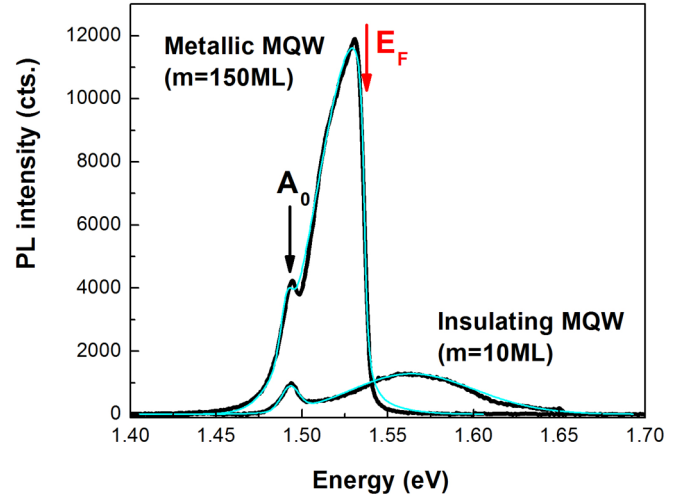


FIG. 1. Photoluminescence spectra measured in metallic ( $m = 150$  ML) and insulating ( $m = 10$  ML)  $(\text{GaAs})_m(\text{Al}_{0.3}\text{Ga}_{0.7}\text{As})_6$  multiple quantum wells at a temperature of 1.6 K. The spectral position of the Fermi level energy for the metallic structure is indicated by the arrow. The results of the fits (explained in the text) are shown by cyan lines.

1.495 eV ( $A_0$ ) is due to recombination of the conduction-band electrons with the holes localized in the neutral C acceptor [9] in the GaAs substrate. The main PL peak is caused by recombination of the conduction-band electrons below the Fermi level with the photoexcited holes. In the insulating 10-ML-wide narrow quantum well the PL peak is blueshifted with respect to the PL peak in the metallic 150-ML-wide quantum well due to the confinement energy. Such blueshifts are evident in the PL spectra of all the samples studied here, presented in Ref. [6]. In the metallic samples the low-energy tail of the main PL peak is composed of localized states formed in both the conduction and valence bands, while the sharp high-energy edge is due to the cutoff Fermi energy. In contrast, in the insulating samples where all the conduction-band electrons occupy localized states, a nearly symmetric broad PL line is observed.

The broadening of the electron and hole states gives rise to the broadening of the high-energy PL edge near the Fermi surface according to Refs. [10,11]:

$$I(\omega) = I_0(\omega) \left[ \frac{1}{2} + \frac{1}{\pi} \arctan(2\tau\delta\Omega) \right], \quad (1)$$

where  $I_0(\omega)$  is the PL intensity represented by a superposition of a disorder-free joint density of states and the exponential low-energy band-tail composed of localized states [12]. A good approximation of such a disorder-broadened low-energy miniband band-tail is the Gaussian function.  $\delta\Omega = \hbar\omega - 2E_F$ , with  $E_F$  being the Fermi energy, and  $\tau$  is the characteristic relaxation time which determines the edge broadening at the Fermi level. This relaxation time is defined by the formula

$$\frac{\hbar}{\tau} = 2\pi(u_e - u_h)^2 N_i \gamma, \quad (2)$$

where  $u_{e(h)}$  is the electron (hole) scattering potential,  $N_i$  is the concentration of imperfections, and  $\gamma$  is the density of

states on the Fermi surface. Formulas (1) and (2) were obtained in the limit  $\hbar/\tau \ll E_F$  for the interaction of electrons with short-range impurity potentials. These assumptions are also valid in the metallic samples studied here with short-range structural disorder potential.

A fit of the spectral shape calculated in this way to the PL measured in the metallic sample allows us to obtain the Fermi level energy shown by the arrow in Fig. 1. The characteristic energy  $\hbar/\tau = 4.8$  meV defined by the electron and hole scattering potentials is found to be responsible for the Fermi level broadening. The same procedure does not apply in the insulating sample where PL emission is presented by a broad line and no Fermi edge cutoff feature is seen. In this case a good fit was obtained with a Gaussian line. In both cases, the  $A_0$  peak was fitted with an additional Gaussian line.

The electron states occupied by the Fermi electrons in the conduction band and the photoexcited holes in the valence band contribute to the optical interband transitions in the form of excitons. Therefore, PL emission reveals features of both bands. However, due to a significant difference between the effective mass of the electrons and the heavy holes in GaAs, in the vicinity of the metal-to-insulator transition which occurs in a system of conduction-band electrons, PL emission from disordered GaAs structures essentially characterizes localization properties of the electrons. Thus, the localization of the conduction-band electrons should dominate the properties of excitons.

The theory of the localized exciton states and their migration over a random potential was developed in Refs. [13,14], which also showed that the macroscopic potential fluctuations and the timescale arguments lead to the exciton mobility edge broadening. Two processes responsible for the PL decay were considered: a direct radiative recombination and an exciton phonon-assisted transfer between localized states. If the phonon-assisted transfer is much faster than the radiative process, then the PL decays with the characteristic time defined by

$$\tau(E) = \frac{\tau_{r0}}{1 + \exp(E - E_c)/\delta E}, \quad (3)$$

where the radiative recombination time  $\tau_{r0}$  is not supposed to change with the emission energy,  $E_c$  is the exciton mobility edge energy, and  $\delta E$  is the characteristic energy of the band-tail density of localized states defined as  $g(E) \sim \exp(-E/\delta E)$ . The exciton lifetime measured in this way in the metallic and insulating samples as a function of the energy was used to determine the exciton mobility edge energy in Ref. [6], and it was attributed to the mobility edge of electrons. As a result, a good correlation between the optical and transport properties was demonstrated in the range close to the MIT.

Strong magnetic field applied to a disordered electron system results in a reduction of the spatial overlap of the electron wave functions which leads to the magnetic-field-induced electron localization [15]. Such modification of the electron wave function should influence the recombination rate of the photoexcited carriers. In the presence of a random potential the effect of the magnetic field is anticipated when a characteristic length of the localization potential is larger than the magnetic length  $l_B = (\hbar/eB)$ . The interface roughness disorder is parameterized by the height  $\Delta$  and the lateral

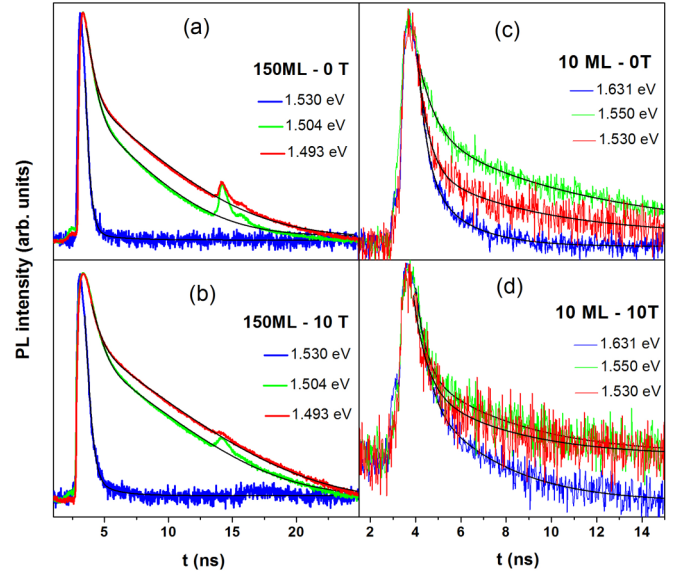


FIG. 2. Photoluminescence transients measured at different energies in (a) and (b) the metallic and (c) and (d) insulating  $(\text{GaAs})_m(\text{Al}_{0.3}\text{Ga}_{0.7}\text{As})_6$  multiple quantum wells at a temperature of 1.6 K in different magnetic fields. Thin black lines show the results of the best fits as explained in the text.

correlation length  $\Lambda$ . When the magnetic field is perpendicular to the interface, a relevant characteristic disorder length is the lateral interface roughness length  $\Lambda$ . An examination of the electron mobility as a function of the quantum well width provides for these interface roughness parameters [16]. In the MQWs studied here we found  $\Delta \approx 0.5$  nm and  $\Lambda \approx 7.5$  nm. These values are in good agreement with the data obtained in similar GaAs/AlAs quantum wells in Ref. [17]. In a magnetic field of 10 T the magnetic length  $l_B \approx 8$  nm is about the lateral interface roughness length. Therefore, such a magnetic field may cause a noticeable effect on the recombination time. With the intention to prove the effect of the magnetic field on the recombination time of the localized electrons we measured the PL transients as a function of the magnetic field.

The characteristic PL transients measured in the metallic and insulating structures are shown in Fig. 2. Small peaks at the time delay of about 14 ns are due to reflections in fiber optics. The best fits of the PL transients  $I_{PL}(t)$  were obtained with two characteristic recombination times, a short time  $\tau_1$  and a long one  $\tau_2$ , according to

$$I_{PL}(t) = A_1 e^{-t/\tau_1} + A_2 e^{-t/\tau_2}, \quad (4)$$

where  $A_{1(2)}$  are the PL amplitudes corresponding to the short- and long-time transients, respectively. Two recombination times point to the presence of two groups of photoexcited carriers which recombine independently. In such a case, it is common to attribute one group to the interband recombination and the other to recombination which involves impurity centers. In our case the valence-band holes and the holes residing on acceptor levels (the neutral C acceptor) recombine with the conduction-band electrons independently, resulting in two rate equations and, as a consequence, in two recombination times.

The PL transients measured in the metallic samples reveal the recombination time, which continually increases with

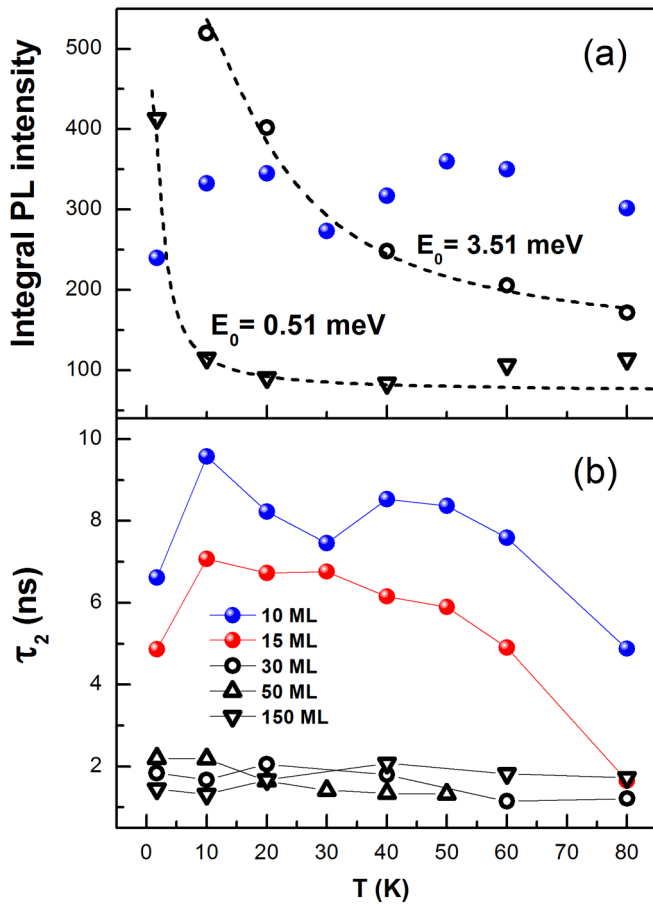


FIG. 3. (a) Integral photoluminescence intensity and (b) the long recombination time  $\tau_2$  measured in  $(\text{GaAs})_m(\text{Al}_{0.3}\text{Ga}_{0.7}\text{As})_6$  MQWs with different quantum well widths as a function of the temperature.

decreasing energy, achieving a saturated value in the energy range of the exponential band-tail states. In this case the temporal response is found to be almost independent of the magnetic field. A more complicated behavior was observed in the insulating sample (10-ML quantum well width): the zero-magnetic-field PL transients display a maximum of the recombination time located near the corresponding PL peak energy, while the applied magnetic field considerably reduces the recombination time, finally making it independent of energy. The details of such a performance of the recombination time in the presence of disorder and the magnetic field are considered below.

As reported above, the recombination time is expected to represent the character of the electron states below the Fermi level. In order to prove the localized nature of the electron states we measured the integral PL intensity and the PL transients in the samples with different disorder strengths as a function of the temperature. The activated character of the integral PL intensity was found in the metallic samples, while no regular variation of the integrated PL intensity was observed in the insulating sample ( $m = 10$  ML) shown in Fig. 3(a). The best fits of the activated dependencies calculated according to the Arrhenius formula  $I_{PL}(T) = I_0/[1 + \exp(-E_0/k_B T)]$ , depicted by dashed lines, result in the activation energies  $E_0 = 3.51$  meV and  $E_0 = 0.51$  meV in the metallic samples with

$m = 30$  and  $150$  ML, respectively. The obtained activation energies directly demonstrate the amplitude of the disorder interface roughness potential increasing with decreasing quantum well width. In the insulating sample the amplitude of the disorder potential is larger than the thermal energy; therefore, the electrons remain localized in the whole interval of the temperature, and the integral PL intensity shows no significant change. The PL transients were measured at the emission energy near the corresponding PL peak. Both short and long recombination times reveal similar behavior. The long recombination time  $\tau_2$  measured in  $(\text{GaAs})_m(\text{Al}_{0.3}\text{Ga}_{0.7}\text{As})_6$  MQWs with different disorder strengths (different quantum well widths  $m$ ) as a function of the temperature is depicted in Fig. 3(b). In the metallic samples ( $m = 30, 50,$  and  $150$  ML) the mobility edge was found well below the Fermi level, while in the metallic sample with strongest disorder ( $m = 15$  ML) and in the insulating sample ( $m = 10$  ML) the position of the mobility edge was determined to be close to the Fermi level [6]. The results presented in Fig. 3 show that the proximity of the mobility edge to the Fermi level is responsible for the observed effect of the temperature. In the metallic regime, where the mobility edge is located significantly below the Fermi level, the temperature does not affect the recombination time because the thermal activation of the electrons residing close to the Fermi level does not change their extended character, while in the insulating regime the elevated temperature results in activation of the localized states below the mobility edge to the extended states above the Fermi level, which gives rise to the increasing recombination rate and, consequently, to the observed drop in the recombination time. As expected, no significant variation of the recombination time with the temperature was found in the metallic samples ( $m = 30, 50,$  and  $150$  ML), while in the metallic sample with strongest disorder ( $m = 15$  ML) and in the insulating sample ( $m = 10$  ML) a significant decrease in the recombination time with the temperature was detected. As mentioned before, the observed decrease in the recombination time is caused by the thermal excitation of the localized electrons, which enhances the electron mobility and thus increases the probability of recombination with the photoexcited holes. It is worth mentioning that according to Refs. [7,16], in a GaAs quantum well the MIT produced by interface roughness scattering is expected at a critical quantum well width of about 5 nm (approximately 18 ML), which agrees well with the data presented in Fig. 3.

The effect of the magnetic field on the PL spectra measured in the metallic and insulating samples is demonstrated in Figs. 4(a) and 4(b), respectively. The PL measured in the metallic sample demonstrates multiple peak structures formed in high magnetic field due to the Landau levels. No significant change in the PL is observed in the insulating sample.

Figure 5 shows the long recombination time  $\tau_2$  determined in the metallic [Figs. 5(a) and 5(b)] and insulating [Fig. 5(c)] MQW structures as a function of the energy, measured in different magnetic fields. Again, similar behavior is found for the short recombination time. The fits of the recombination time calculated according to Eq. (3) to the data presented in Fig. 5 were used to extract the corresponding mobility edges  $E_c$ , while the fits of the high-energy PL edge according to Eq. (1) were employed to obtain the Fermi levels  $E_F$  in the metallic samples. Due to the low mobility and, as a

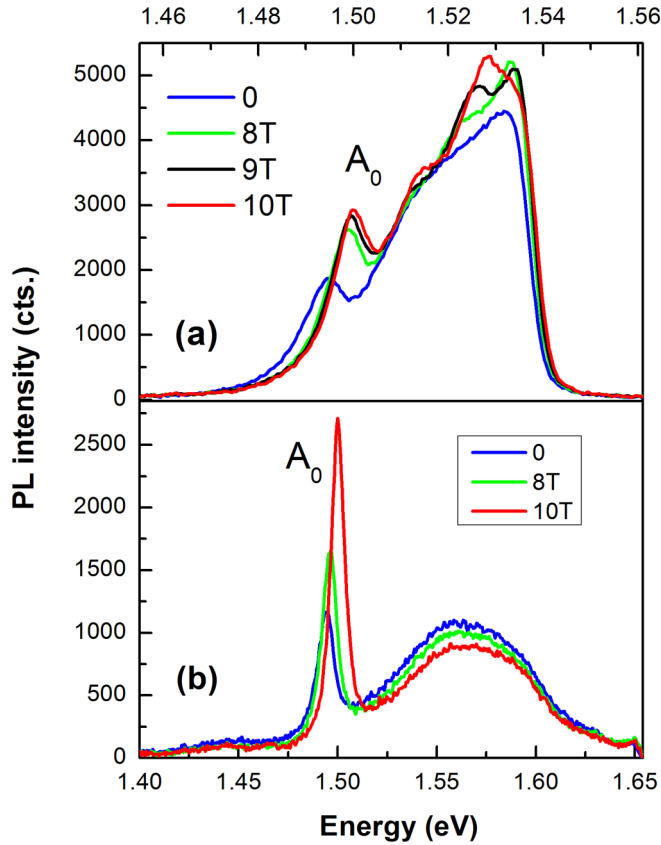


FIG. 4. Photoluminescence spectra measured in (a) metallic ( $m = 150$  ML) and (b) insulating ( $m = 10$  ML)  $(\text{GaAs})_m(\text{Al}_{0.3}\text{Ga}_{0.7}\text{As})_6$  multiple quantum wells at a temperature of 1.6 K in different magnetic fields.

consequence, the large broadening of the Fermi edge, we were not able to determine the Fermi level in the narrow quantum well width samples (10 and 15 ML) where the PL emission takes the form of a broad Gaussian-like peak. However, the identical uniform doping in all the samples studied here should result in the same electron concentration. Therefore, the Fermi level is anticipated to not change considerably from sample to sample. As mentioned above, the PL peaks measured in the quantum wells with different widths are blueshifted due to the confinement energy. The quantum confinement results in a corresponding apparent shift of the Fermi level energy obtained with the fit using Eq. (1). Therefore, the apparent Fermi level energies found in the narrow quantum wells are larger than those obtained in the wide quantum wells. An estimated difference between the confinement energies is about 0.1 eV, which is roughly consistent with the observed PL shift. The interval where the apparent Fermi levels were obtained in the metallic quantum wells is shown in Fig. 5 by the hatched area. Based on the arguments given above, we conclude that in the 10-ML quantum well width insulating sample the Fermi level resides close to the corresponding mobility edge energy. This is in agreement with the insulating character of this sample proven in the magnetotransport measurements [8], which implies  $E_c \geq E_F$ .

As shown in Figs. 5(a) and 5(b), in the metallic samples with the 150- and 15-ML quantum well widths, the recombination

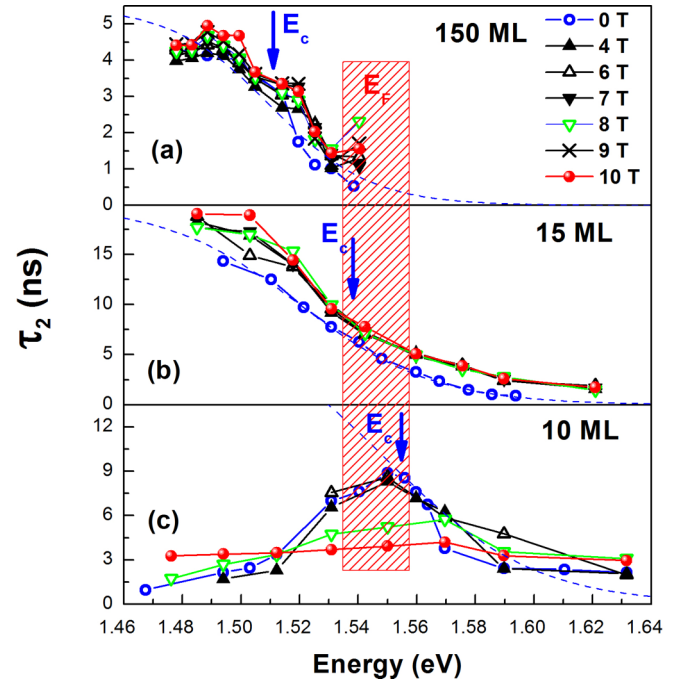


FIG. 5. Long recombination time measured in the metallic (a,b) and insulating (c)  $(\text{GaAs})_m(\text{Al}_{0.3}\text{Ga}_{0.7}\text{As})_6$  multiple quantum wells as a function of the energy in different magnetic fields. The positions of the Fermi levels  $E_F$  were determined in zero magnetic field, as explained in the text. The hatched area shows the interval of Fermi levels obtained in the metallic quantum wells. Dashed lines show the results of the best fits according to Eq. (3) and the corresponding mobility edge energy  $E_c$  obtained in the case of zero magnetic field.

time follows the dependence on the energy defined by Eq. (3), which was used to obtain the values of mobility edge energies in all the samples. A small blueshift of the mobility edge observed in these samples with increasing magnetic field is due to the magnetic-field-induced energy shift  $0.5\hbar\omega_c$  (where  $\omega_c$  is the cyclotron frequency), which in GaAs at 10 T is about 8.5 meV. In the metallic regime the mobility edge is found below the Fermi level. The decreasing quantum well width and as a consequence, increasing disorder strength result in the increasing mobility edge energy and in an overall rise in the radiative recombination time. Both the recombination time and the mobility edge energy increase with increasing disorder because the number of localized electrons increases and spreads over a larger energy interval. In contrast to the results obtained in the wide quantum well metallic structures, in the insulating structure with the smallest quantum well width (10 ML) shown in Fig. 5(c), the mobility edge is placed above or in close proximity to the Fermi level, and the recombination time reveals a maximum at the energy corresponding to the mobility edge. In the case of such strong disorder the recombination time decreases below the mobility edge due to disorder-induced relaxation of the momentum selection rule, which enhances the probability of recombination of the localized electrons.

As shown in Fig. 5(c), in the insulating sample the magnetic field drastically reduces the recombination time at the

maximum. As a consequence, in a strong magnetic field the recombination time was found to be independent of the energy. Such an effect of the magnetic field on radiative recombination time is consistent with the magnetic-field-induced electron localization cited above, which favors relaxation of the momentum selection rule. The relaxation of the selection rule leads to the increasing probability of electron-hole radiative recombination and thus to the observed decreasing recombination time.

#### IV. CONCLUSION

A transition from localized to extended electron states below the Fermi level was studied in the multiple narrow quantum well GaAs/AlGaAs heterostructures. Decreasing the quantum well width enhances disorder due to interface roughness and, as a consequence, results in the metal-insulator transition. The time-resolved photoluminescence enabled us to determine the energy of the mobility edge separating the localized and extended electron states. As expected, the mobility edge was found below the Fermi level in the metallic regime, while in the insulating one it was located above the Fermi level. Close similarities were observed in the temporal response of the disordered electrons below the Fermi level and the response

of the conducting electrons subjected to a disorder potential, usually observed in electric transport measurements. That is, the recombination time measured in the metallic regime does not reveal a noteworthy change with the temperature, while the thermal activation of the localized electrons causes a faster recombination with increasing temperature. A unique effect of the magnetic field on relaxation of the momentum conservation rule in the presence of strong localization was observed: the magnetic-field-induced reduction of the spatial overlap of the localized electron wave functions results in a relaxation of the momentum conservation rule. Thus, time-resolved photoluminescence measurements provide insights into the evolution of the localized electron states below the Fermi level which are inaccessible with electric transport measurements. The demonstrated technique may be used as a tool to explore complicated physics related to the metal-insulator transition in a system with a fixed disorder and Coulomb interaction.

#### ACKNOWLEDGMENTS

Financial support from the Brazilian agencies Fundação de Amparo à Pesquisa do Estado de São Paulo and Conselho Nacional de Desenvolvimento Científico e Tecnológico is gratefully acknowledged.

- 
- [1] E. Miranda and V. Dobrosavljević, *Rep. Prog. Phys.* **68**, 2337 (2005).
  - [2] V. Dobrosavljević, in *Conductor Insulator Quantum Phase Transitions*, edited by V. Dobrosavljević, N. Trivedy, and J. M. Valles, Jr. (Oxford University Press, Oxford, 2012), p. 4.
  - [3] S. Sachdev, *Quantum Phase Transitions*, 2nd ed. (Cambridge University Press, Cambridge, 2011).
  - [4] N. F. Mott, *J. Non-Cryst. Solids* **8–10**, 1 (1972).
  - [5] M. H. Cohen, *J. Non-Cryst. Solids* **4**, 391 (1972).
  - [6] M. A. Tito and Y. A. Pusep, *Superlattices Microstruct.* **104**, 156 (2017).
  - [7] A. Gold, *Solid State Commun.* **60**, 531 (1986).
  - [8] Y. A. Pusep, H. Arakaki, and C. A. de Souza, *Phys. Rev. B* **68**, 205321 (2003).
  - [9] L. Pavesi and M. Guzzi, *J. Appl. Phys.* **75**, 4779 (1994).
  - [10] E. G. Batyev, Yu. A. Pusep, and M. P. Sinyukov, *Sov. Phys. Solid State* **27**, 708 (1985).
  - [11] Y. A. Pusep, F. E. G. Guimaraes, M. B. Ribeiro, H. Arakaki, C. A. de Souza, S. Malzer, and G. H. Döhler, *Phys. Rev. B* **70**, 092301 (2004).
  - [12] F. Urbach, *Phys. Rev.* **92**, 1324 (1953).
  - [13] E. Cohen and M. D. Sturge, *Phys. Rev. B* **25**, 3828 (1982).
  - [14] G. Gourdon and P. Lavallard, *Phys. Status Solidi B* **153**, 641 (1989).
  - [15] B. I. Shklovskii and A. L. Efros, *Electron Properties of Doped Semiconductors*, Solid State Physics Vol. 45 (Springer, Berlin, 1984).
  - [16] A. Gold, *Phys. Rev. B* **35**, 723 (1987).
  - [17] H. Sakaki, T. Noda, K. Hirakawa, M. Tanaka, and T. Matsusue, *Appl. Phys. Lett.* **51**, 1934 (1987).